

Document downloaded from:

<http://hdl.handle.net/10251/109083>

This paper must be cited as:

Garcia-Garcia, F.; Valls-Ayuso, A.; Benlloch Marco, J.; Valcuende Payá, MO. (2017). An optimization of the work disruption by 3D cavity mapping using GPR: A new sewerage Project in Torrente (Valencia, Spain). *Construction and Building Materials*. 154:1226-1233. doi:10.1016/j.conbuildmat.2017.06.116



The final publication is available at

<https://doi.org/10.1016/j.conbuildmat.2017.06.116>

Copyright Elsevier

Additional Information

Manuscript Number:

Title: An optimization of the work disruption by 3D cavity mapping using GPR: A new sewerage project in Torrente (Valencia, Spain)

Article Type: VSI:GPR & NDTs in Civil Eng

Keywords: street work disruption; ground-penetrating radar; GPR; cavity; cave hazards; 3D mapping; sewerage project

Corresponding Author: Dr. Ana Valls Ayuso, Ph.D.

Corresponding Author's Institution: Polytechnic University of Valencia

First Author: Francisco Garcia-Garcia, Professor

Order of Authors: Francisco Garcia-Garcia, Professor; Ana Valls Ayuso, Ph.D.; Javier Benlloch-Marco, Professor; Manuel Valcuende-Paya, Professor

Abstract: This paper describes the inspection for cavity detection in an urban area in Torrente (Valencia, Spain). A shallow cavity was found during excavation works for a sewerage project. Digging activities were stopped immediately and a GPR survey was required to reorganize the sewerage planning. The 3D GPR-mapping pinpointed cavities mostly on one side of the street. As a result, the sewerage system layout was moved to the side of the street where poor cavity evidences were detected. GPR technique is helpful for minimizing costs, time, work safety risks and inconveniences to neighborhood during civil engineering works, especially in urbanized areas.

Suggested Reviewers: Vivian W. Y. Tam  
University of Western Sydney  
V.Tam@westernsydney.edu.au

Jose Luis Ponz Tienda  
Universidad de los Andes, Colombia  
jl.ponz@uniandes.edu.co

Vega Pérez Gracia  
Polytechnic University of Catalonia  
vega.perez@upc.edu

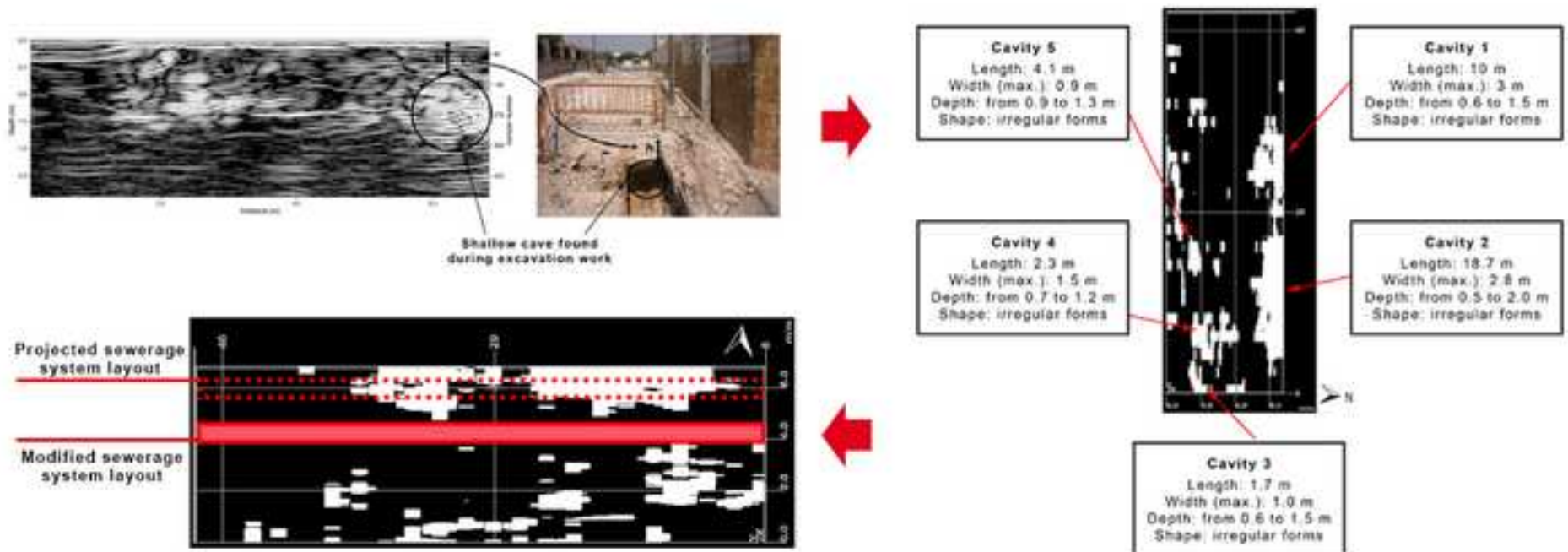
Petros Patias  
The Aristotle University of Thessaloniki  
patias@auth.gr

Federica Sandrone  
Ecole polytechnique fédérale de Lausanne  
federicalucia.sandrone@epfl.ch

## 1 **Highlights**

- 2 • 3D GPR data has been used for cavity detection in urbanized areas.
- 3 • 3D representations of GPR data facilitate interpretation in civil engineering.
- 4 • GPR survey reduces work safety risks in urbanized karst hazardous areas.
- 5 • Civil engineering projects including GPR are cost-effective and time-reducing.

## GPR AS A TOOL FOR MINIMIZING STREET WORK DISRUPTION IN URBANIZED AREAS





24 **Keywords**

25 street work disruption; ground-penetrating radar; GPR; cavity; cave hazards; 3D  
26 mapping; sewerage project

27

28 **1. Introduction**

29 Civil engineering works requires accurate techniques for cavity detection in urbanized  
30 areas. Non-destructive techniques (NDT) offer multiple possibilities for the  
31 documentation and interpretation of underground anomalies and structures. Geophysics  
32 is successfully employed for non-invasive explorations in all fields of civil engineering.  
33 It provides non-destructive effective solutions and offers significant information.

34 The most employed geophysical methods for mapping the subsurface space are: (a) the  
35 electrical and electromagnetic resistivity methods, (b) the seismic methods and (c) the  
36 gravimetric methods [1]. Each geophysical technique has its pros and cons.  
37 Microgravity is one of the most reliable techniques for the detection and outline of  
38 subterranean anomalies [2-4]. However, data acquisition and result analysis involve  
39 long processing time. The electrical resistivity [5] and the magnetic methods can offer  
40 excellent results [6,7], but they provide less information, because of their low resolution  
41 in the three-dimensional (3D) images. The seismic methods have been used to locate  
42 subterranean structures [8,9]. Nevertheless, this technique shows some limitations in the  
43 peripheral sectors, where the angular coverage limitation derives in poor results. The  
44 ground-penetrating radar (GPR) method is often a more effective means in the study of  
45 underground structures than other geophysical methods. Currently, it is the dominant  
46 technology for location surveys. This technique is a useful mapping tool due to its  
47 suitability for high-resolution subsurface imaging and 3D data representation. It allows

48 attaining reliable results, ensures complete coverage of the site and, therefore, increases  
49 the survey effectiveness and reduces costs [10].

50 This technique has been widely applied for mapping the underworld [11], focusing on  
51 utility location [12-14], road maintenance [15-17] and inspection of natural or man-  
52 made underground structures [18-21]. There have also been published studies on  
53 imaging of collapsed underground systems in natural and urban areas [22,23]. Air-filled  
54 cavities reflect the electromagnetic wave with maximum relative amplitudes at the top  
55 of the cavity on a GPR section. So, this method is usually employed for non-destructive  
56 detection of cavities in karst areas with special attention to those located in urbanized  
57 zones [24-29].

58 Civil engineering projects aim at reducing safety risks and cost risks, especially in street  
59 works. Clients request high levels of accuracy, while surveyors have interest in  
60 effectivity and high quality of the location survey to ensure client confidence. Street  
61 work disruption results in economic and management drawbacks [30]. The accuracy in  
62 pinpointing subsurface structures and defining their geometry provide additional  
63 information to design and perform maintenance and new projects by minimizing  
64 potential errors [31]. The GPR method is proposed in this study due to its high  
65 resolution subsurface imagery, fast data acquisition and suitability for detecting and  
66 mapping buried anomalies.

67 In order to evaluate the effectiveness of the GPR technique for cave detection in  
68 urbanized areas, a sector of a housing development was analyzed. Prior to this study, a  
69 shallow cave was found during sewerage excavation work. Given the nature of the  
70 urban project location, cave evidences and indicators were masked. The aim of this  
71 work is twofold: first, to pinpoint cave hazards in a street using 3D GPR data  
72 visualization with iterative depth and profile slice and second, to prove that GPR is a

73 time and cost-effective method for civil engineering works and urban planning. As a  
74 result of this study 5 cavities were detected with a volume greater than 1 m<sup>3</sup> in irregular  
75 forms and depths, and several smaller ones were identified.

76

## 77 **2. Site description**

78 The study area is situated in Torrente, a town located 12 km southwest of Valencia city  
79 (Fig. 1). Valencia is located at the Spanish Mediterranean shore. Torrente is placed on  
80 Tertiary formations that border with alluvial sediments and flooding silt from the River  
81 Turia. These Tertiary formations emerge in western and southwestern areas, where they  
82 form the first limestone foothills [32,33].

83 Torrente population growth (more than 80,000 inhabitants last year) has caused urban  
84 development southwards from its downtown. New urbanized areas are located in  
85 mountains composed of fractured limestone with presence of karst activity. The studied  
86 zone is located in this setting, where housing estates were built. The need to expand the  
87 sewerage system in the area resulted in a civil engineering street work. Urbanized areas  
88 in karst hazardous zones suffer from infrastructure jeopardy, which usually implies  
89 economic losses. During street excavation work, a shallow cave was found. This fact  
90 resulted in digging activity stoppage. Therefore, a GPR survey was required for cavity  
91 detection in order to minimize street work disruption and reduce safety risks and cost  
92 risks.

93

94 Fig. 1

95

96



## 97 **3. Materials and Methods**

### 98 **3.1. Field data acquisition**

99 Data collection was required from the whole street under study. A profile grid 2x2 m  
100 was carried out on the street (Fig. 2). So, three-dimensional (3D) GPR methodologies  
101 were performed for pinpointing and defining underground karst activity. The GPR data  
102 were collected using a GSSI SIR-3000 equipment with a nominal 400 MHz centre  
103 frequency antenna within a total time window of 60 ns.

104

105 Fig. 2

106

### 107 **3.2. Data processing**

108 Preliminary excavation works unveiled a shallow karst cave and expose a cross-  
109 sectional image of the street (Fig. 3). The reflection from the top of this shallow karst  
110 was recorded at the end of profile P3 line. It was used as a calibration to collect the karst  
111 zone data. So the soil thickness over the cavity distance (h) could be measured. This  
112 value in addition to the two-way travel time (t) defined by GPR measurements allowed  
113 calculating the dielectric permittivity ( $\epsilon$ ) according to the following equation [34-36]:

$$114 \quad \epsilon_r = \left(\frac{c}{v}\right)^2 = \left(\frac{ct}{2h}\right)^2 \quad (1)$$

115 For time scale to depth conversion, the subsurface electromagnetic wave velocity was  
116 obtained from  $\epsilon$  [35,36]. An average velocity of 0.084 m/ns for limestone medium was  
117 obtained from the following equation:

$$v = \frac{2 \cdot h}{t} \quad (2)$$

118

119

120 Fig. 3

121

### 122 **3.3. 3D modeling**

123 RADAN software was used for data processing. As a first stage, time zero correction,  
124 background removal and gaining function were also applied with the aim at amplifying  
125 the received signal and improving anomaly identification. Also 2D raw data were  
126 processed by applying filters such as Kirchhoff migration filter using the average  
127 velocity for diffraction removal.

128 A GPR-3D model of the subsurface was obtained by aligning processed 2D profiles in  
129 order to pinpoint cavity evidences beneath the street under study. Several amplitude  
130 slice maps were obtained at different levels for mapping the subsurface to the maximum  
131 depth of 1.5 m projected excavation for sewer pipe. Amplitude slice maps from the 3D  
132 model were used to identify irregularities at a constant depth. Besides, transparent  
133 visualization of the 3D GPR data set was conducted for revealing main subsurface  
134 anomalies.

135 The main objective was to define the location, shape and depth of the cavities detected.  
136 The results can be enriched when visualized as a volumetric rendering. This procedure  
137 allows anyone to reckon and understand how the subsurface area under study looks.  
138 Maps and 3D representations allow for the characterization of the radar data, for

139 geometrical dimensioning of the cavities as well as for a better understanding of the  
140 electromagnetic results for clients and civil engineering employees.

141

#### 142 **4. Results**

143 Radargram profiles showcase an overview of the site under study. Fig. 4 includes the  
144 three 2D longitudinal profiles acquired along the street. These radargrams illustrate the  
145 subsurface dissimilarities on different sections of the street. The southern profile shows  
146 scarce subsurface anomalies, while the central radargram along the street displays subtle  
147 features that may correspond with karst activity from meters 0 to 16 at a depth of 1.5 m.  
148 The northern longitudinal 2D profile indicates the strongest reflectors regarding the  
149 underground cavities. From meter 0 to meter 32 at a depth between 0.5 and 2 m,  
150 subsurface cavities are identified in Fig. 4.a).

151

152 Fig. 4

153

154 However, defining geometrical and dimensional features of caves from the GPR 2D  
155 data is time-consuming and requires an individual analysis of every radargram. 3D  
156 visualization techniques were applied to overcome this difficulty. Fig. 5.a) illustrates a  
157 set of selected depth-slices derived from the GPR 3D cube. The most representative  
158 depth-slices are identified at 0.5, 1.0, 1.5 and 2.0 meter-depth. The maximum and  
159 minimum amplitude ranges according to the amplitude-color scale characterize the  
160 cavities filled with air in the subsurface study site. Moreover, the isosurface rendering  
161 technique enabled visualizing the whole subterranean structures defined by karst

162 activity, as shown in Fig. 5.b). The color restriction made only cavities visible and  
163 simplified cavity detection and data interpretation. Hence, it was possible to crosscheck  
164 both depth ranges and isosurface ranges and in order to determine the exact location of  
165 the subsurface karst activity and to dimension the cavities by defining their extension  
166 and depth-positioning. The 3D GPR data revealed 5 cavities with a volume greater than  
167  $1 \text{ m}^3$  in irregular shapes between 0.5 and 2.0 meter deep and several smaller ones.

168

169 Fig. 5

170

171 The GPR 3D data visualizations have improved the application of GPR for civil  
172 engineering prospections. In this particular case, GPR has aided in characterizing the  
173 underground karst structures for minimizing street work disruption. Despite its  
174 contribution, the interpretation of radargrams is not a simple task for non-geophysicists.  
175 In the civil engineering field, isosurface 3D modeling result in a better understanding of  
176 the outcomes derived from the GPR data. Location and general dimensions of the  
177 subsurface structures can be defined in order to characterize the detected 5 cavities in  
178 the site under study (Fig. 6).

179

180 Fig. 6

181

182 As seen in the Figures 5 and 6, the karst activity was mainly concentrated in the  
183 northern area of the street under study. This part of the street was supposed to include

184 the sewerage layout. However, the detection of subterranean structures led to a  
185 modification of the civil engineering project. The 3D GPR data helped in the decision-  
186 making for modifying the sewerage system layout where fewer cavities with smaller  
187 dimensions were identified. So the sewerage system layout was moved to the side of the  
188 street where poor cavity evidences were detected, as shown in Fig. 7.

189

190 Fig. 7

191

## 192 **5. Discussion and conclusions**

193 Civil engineering projects usually focus on street work. Effectiveness, high level of  
194 accuracy and quality are terms to bear in mind when planning civil engineering surveys.  
195 However, problems usually arise during street work carrying out. This fact implies a  
196 delay in the project and an extension of the street work disruption. And hence, it can  
197 result in economic and management drawbacks.

198 This situation took place in the project presented in this study. The accidental discovery  
199 of cavities karst involved holdup of field work. Therefore, Geophysics experts were  
200 required to perform a survey of the underground. The aim was at identifying if it was  
201 possible to continue with the sewerage project as it was planned or if it was necessary to  
202 redirect the facility layout. The GPR results revealed the existence of cavities in the  
203 planned area for sewerage facilities, so it was necessary to modify the layout of the  
204 project. It all not only involved an extension in time but also an additional cost derived  
205 from the hiring of Geophysics experts, the equipment rental and especially from the

206 street work disruption in an urbanized area causing unnecessary inconvenience to  
207 neighborhood.

208 These drawbacks can be anticipated and solved efficiently. For this purpose,  
209 geophysical prospections should be included in the preliminary studies of civil  
210 engineering projects. This way, unnecessary costs could be avoided and street work  
211 disruption could be significantly reduced in urbanized areas. Moreover, prior  
212 examination of the underground can minimize the potential for errors and increase the  
213 efficiency in field work.

214 We produced images of the underground in an urbanized area via a proposed method  
215 based on 3D visualization of the GPR data. This allowed us to reveal and differentiate  
216 subsurface cavities from the surrounding soil medium.

217 The transparent 3D imaging successfully allowed the identification of targets (cavities)  
218 in the underground, providing accurate locations and depths. The isosurface 3D  
219 modeling derived from the GPR data provided better imaging to accurately interpret the  
220 subsurface by non-geophysicists professionals that work in the civil engineering field.  
221 So these data helped them in the decision-making for modifying the sewerage system  
222 layout. The results demonstrated that the GPR method and the 3D visualization can give  
223 perfect outcomes in a delimited urbanized area.

224 We conclude that the GPR technique provides highly accurate results for the position  
225 and depth of cavities within civil engineering projects in urbanized areas. 3D GPR  
226 survey reduces work safety risks in urbanized karst hazardous areas. Mapping cavities  
227 within urban areas is cost-effective and time-reducing, especially regarding street work  
228 disruption.

229

230

231 **Acknowledgements**

232 This research did not receive any specific grant from funding agencies in the public,  
233 commercial, or not-for-profit sectors.

234

235 **References**

236 [1] D.K. Butler, Detection and characterization of subsurface cavities, tunnels and  
237 abandoned mines, in: Near-surface geophysics and human activity. Proceedings of  
238 the 3rd International Conference on Environmental and Engineering Geophysics  
239 (ICEEG), Science Press USA, Monmouth Junction, New Jersey, 2008, pp. 578-  
240 584.

241 [2] D.K. Butler, Microgravimetric and gravity gradient techniques for detection of  
242 subsurface cavities. *Geophysics* 49 (1984) 1084-1096.

243 [3] I. Rodríguez-Abad, F. García-García, I. Rodríguez-Abad, M. Ramírez-Blanco, J.L.  
244 Montalvá-Conesa, J. Benlloch-Marco, R. Capuz-Lladró, Non-destructive  
245 assessment of a buried rainwater cistern at the Carthusian Monastery ‘Vall de  
246 Crist’(Spain, 14th century) derived by microgravimetric 2D modeling, *J. Cult.*  
247 *Herit.* 8 (2007) 197-201.

248 [4] D.E. Yule, M.K. Sharp, D.K. Butler, Microgravity investigations of foundation  
249 conditions. *Geophysics* 63 (1998) 95-103.

- 250 [5] F.J. Martínez-Moreno, J. Galindo-Zaldívar, A. Pedrera, L. González-Castillo,  
251 Detecting gypsum caves with microgravity and ERT under soil water content  
252 variations (Sorbas, SE Spain), *Eng. Geol.* 193 (2015) 38-48.
- 253 [6] H. Becker, J.W. Fassbinder, Magnetic prospecting in archaeological sites, ICOMOS,  
254 2001.
- 255 [7] H. von der Osten-Woldenburg, B. Chaume, W. Reinhard, Magnetic imaging of a  
256 late Bronze Age tumulus in France before and during excavation, *The Leading*  
257 *Edge* 21 (2002) 465-466.
- 258 [8] L. Polymenakos, S. Papamarinopoulos, A. Liossis, C. Koukouli-Chryssanthaki,  
259 Investigation of a monumental Macedonian tumulus by three-dimensional seismic  
260 tomography, *Archaeol. Prospect.* 11 (2004) 145-158.
- 261 [9] G.N. Tsokas, C.B. Papazachos, A. Vafidis, M.Z. Loukoyiannakis, G. Vargemezis,  
262 K. Tzimeas, The detection of monumental tombs buried in tumuli by seismic  
263 refraction, *Geophysics* 60 (1995) 1735-1742.
- 264 [10] D.J. Daniels, *Ground Penetrating Radar*, The Institution of Electrical Engineers,  
265 Herts, UK, 2004.
- 266 [11] C.D.F. Rogers, D.N. Chapman, N. Metje, Mapping the underworld - UK utilities  
267 mapping, in: *Proceedings of the 11th International Conference on Ground*  
268 *Penetrating Radar (GPR2006)*, Columbus, Ohio, USA. 2006.
- 269 [12] M. Metwaly, Application of GPR technique for subsurface utility mapping: A case  
270 study from urban area of Holy Mecca, Saudi Arabia, *Measurement* 60 (2015) 139-  
271 145.



- 272 [13] J.L. Porsani, Y.B. Ruy, F.P. Ramos, G.R. Yamanouth, GPR applied to mapping  
273 utilities along the route of the Line 4 (yellow) subway tunnel construction in São  
274 Paulo City, Brazil, *J. Appl. Geophys.* 80 (2012) 25-31.
- 275 [14] S.W. Jaw, M. Hashim, Locational accuracy of underground utility mapping using  
276 ground penetrating radar, *Tunn. Undergr. Sp. Tech.* 35 (2013) 20-29.
- 277 [15] A. Benedetto, A three dimensional approach for tracking cracks in bridges using  
278 GPR, *J. Appl. Geophys.* 97 (2013) 37-44.
- 279 [16] J. Pedret Rodés, V. Pérez-Gracia, A. Martínez-Reguero, Evaluation of the GPR  
280 frequency spectra in asphalt pavement assessment, *Constr. Build. Mater.* 96  
281 (2015) 181–188.
- 282 [17] T. Saarenketo, T. Scullion, Road evaluation with ground penetrating radar, *J. Appl.*  
283 *Geophys.* 43 (2000) 119-138.
- 284 [18] Ó. Pueyo-Anchuela, A. Pocoví Juan, M.A. Soriano, A.M. Casas-Sainz,  
285 Characterization of karst hazards from the perspective of the doline triangle using  
286 GPR - Examples from Central Ebro Basin (Spain), *Eng. Geol.* 108 (2009) 225–  
287 236.
- 288 [19] J.A. Doolittle, N.F. Bellantoni, The search for graves with ground-penetrating radar  
289 in Connecticut, *J. Archaeol. Sci.* 37 (2010) 941–949.
- 290 [20] X. Núñez-Nieto, M. Solla, A. Novo, H. Lorenzo, Three-dimensional ground-  
291 penetrating radar methodologies for the characterization and volumetric  
292 reconstruction of underground tunneling, *Constr. Build. Mater.* 71 (2014) 551–  
293 560.

- 294 [21] T.C. Yang, J.X. Feng, Z.J. Wang, The application of GPR to the exploration of  
295 karst caves in the foundation of bridge tower and its signal analysis, *Geophys.*  
296 *Geochem. Explor.* 35 (2011) 280–284.
- 297 [22] J. Andrade dos Reis Jr, D. Lopes de Castro, T.E. Silva de Jesus, F. Pinheiro Lima  
298 Filho, Characterization of collapsed paleocave systems using GPR attributes, *J.*  
299 *Appl. Geophys.* 103 (2014) 43–56.
- 300 [23] Y. Jeng, C.-S. Chen, Subsurface GPR imaging of a potential collapse area in urban  
301 environments, *Eng. Geol.* 147-148 (2012) 57–67.
- 302 [24] A. Billi, L. De Filippis, P.P. Poncia, P. Sella, C. Faccenna, Hidden sinkholes and  
303 karst cavities in the travertine plateau of a highly-populated geothermal seismic  
304 territory (Tivoli, central Italy), *Geomorphology* 255 (2016) 63–80.
- 305 [25] A.L. Fernandes Jr., W.E. Medeiros, F.H.R. Bezerra, J.G. Oliveira Jr., C.L. Cazarin,  
306 GPR investigation of karst guided by comparison with outcrop and unmanned  
307 aerial vehicle imagery, *J. Appl. Geophys.* 112 (2015) 268–278.
- 308 [26] F.J. Martinez-Moreno, J. Galindo-Zaldívar, A. Pedrera, T. Teixido, P. Ruano, J.A.  
309 Peña, L. González-Castillo, A. Ruiz-Constán, M. López-Chicano, W. Martín-  
310 Rosales, Integrated geophysical methods for studying the karst system of Gruta de  
311 las Maravillas (Aracena, Southwest Spain), *J. Appl. Geophys.* 107 (2014) 149-  
312 162.
- 313 [27] Ó. Pueyo Anchuela, P. López Julián, A.M. Casas Sainz, C.L. Liesa, A. Pocoví  
314 Juan, J. Ramajo Cordero, J.Á. Pérez Benedicto, Three dimensional  
315 characterization of complex mantled karst structures. Decision making and

- 316 engineering solutions applied to a road overlying evaporite rocks in the Ebro  
317 Basin (Spain), *Eng. Geol.* 193 (2015) 158-172.
- 318 [28] Ó. Pueyo Anchuela, A.M. Casas Sainz, A. Pocoví Juan, H. Gil Garbí, Assessing  
319 karst hazards in urbanized areas. Case study and methodological considerations in  
320 the mantle karst from Zaragoza city (NE Spain), *Eng. Geol.* 184 (2015) 29–42.
- 321 [29] K. Samyn, F. Mathieu, A. Bitri, A. Nachbaur, L. Closset, Integrated geophysical  
322 approach in assessing karst presence and sinkhole susceptibility along flood-  
323 protection dykes of the Loire River, Orléans, France, *Eng. Geol.* 183 (2014) 170–  
324 184.
- 325 [30] A.M. Thomas, C.D.F. Rogers, D.N. Chapman, N. Metje, J. Castle, Stakeholder  
326 needs for ground penetrating radar utility location, *J. Appl. Geophys.* 67 (2009)  
327 345–351.
- 328 [31] Y. Yuan, J. Xiaomo, L. Xian, Predictive maintenance of shield tunnels, *Tunn.*  
329 *Undergr. Sp. Tech.* 38 (2013) 69–86.
- 330 [32] V. Díaz Del Río, J. Rey, R. Vegas, The Gulf of Valencia continental shelf:  
331 Extensional tectonics in Neogene and Quaternary sediments, *Mar. Geol.* 73  
332 (1986) 169-179.
- 333 [33] M.T. Bartrina, L. Cabrera, M.J. Jurado, J. Guimerá, E. Roca, Evolution of the  
334 central Catalan margin of the Valencia trough (western Mediterranean).  
335 *Tetono physics* 203 (1992) 219-247.
- 336 [34] L.B. Conyers, *Ground-Penetrating Radar for Archaeology*, Oxford, U.K., AltaMira  
337 Press, 2013.

338 [35] F. García, Aplicaciones de la técnica geofísica de prospección por georradar en  
339 ingeniería civil y glaciología, Ph.D. dissertation, Polytechnic Univ. Catalonia,  
340 Barcelona, Spain, 1997.

341 [36] V. Pérez, Radar del subsuelo. Evaluación en arqueología y en patrimonio histórico-  
342 artístico, Ph.D. dissertation, Polytechnic Univ. Catalonia, Barcelona, Spain, 2001.

343

344 **Figure captions**

345

346 Fig. 1. Geographical location of the study site (Torrente, Valencia, Spain), where we  
347 can observe urbanized areas and plots of undeveloped land.

348

349 Fig. 2. Prospection area and GPR data acquisition in the site under study: a profile grid  
350 2x2 m (22 transversal and 3 longitudinal profiles).

351

352 Fig. 3. The reflection from the top of the shallow karst at the end of the P3 profile line  
353 was used as a calibration to calculate an average velocity for this study. a) Radargram of  
354 the GPR profile P3: shallow cavity between meter 5.3 and meter 7.7 at 0.50 m-depth. b)  
355 Detailed image from the study site showing the cavity depth found during the  
356 excavation work for the sewerage project.

357

358 Fig. 4. a) Radargram profile P24 (northern area of the study site). b) Radargram profile  
359 P23. c) Radargram profile P25 (southern area). d) Profiles P25, P23 and P24, showing  
360 strong subsurface cavity evidences in P24 and less presence of karst activity in P25.

361

362 Fig. 5. a) Solid depth slices obtained from the 3D cube created, at 0.5, 1.0, 1.5 and 2.0  
363 meter-depth. b) Isosurfaces showing 5 detected cavity structures with a volume greater  
364 than 1 m<sup>3</sup> and several smaller ones.

365

366 Fig. 6. Isosurface generated from overlay analysis considering the whole set, where the  
367 general features of the detected cavities are defined.

368

369 Fig. 7. The modified sewerage system layout according to the isosurface derived from  
370 GPR data.

371



Figure 2  
[Click here to download high resolution image](#)





**Figure 3**  
[Click here to download high resolution image](#)

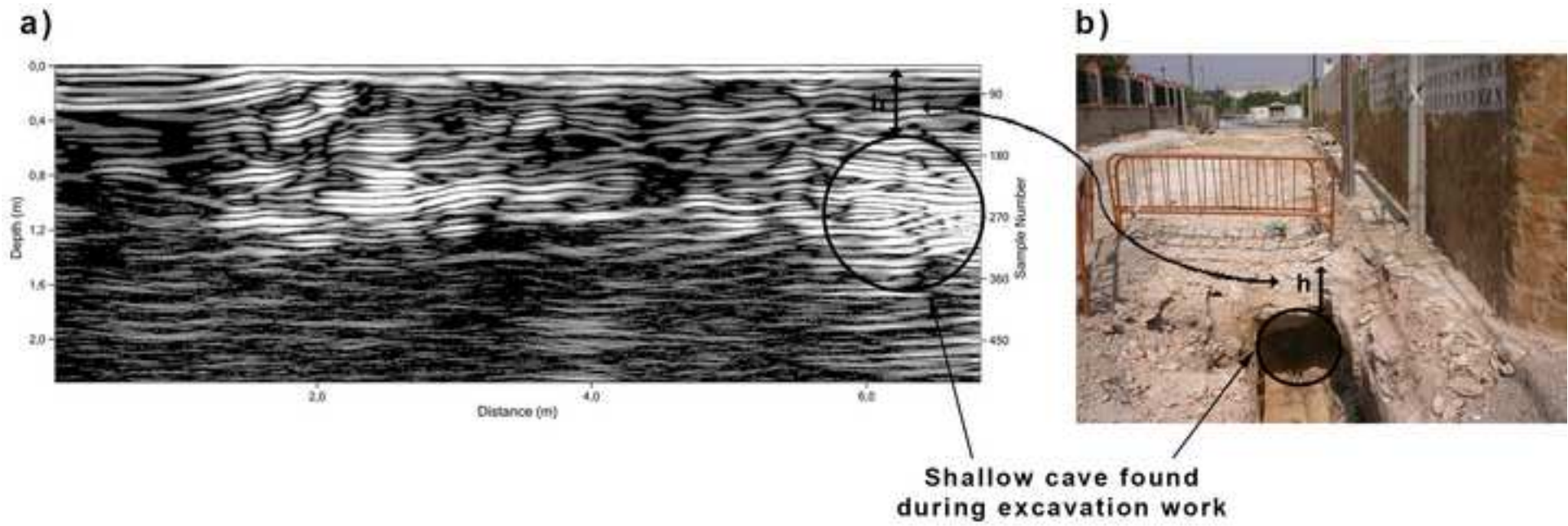


Figure 4  
[Click here to download high resolution image](#)

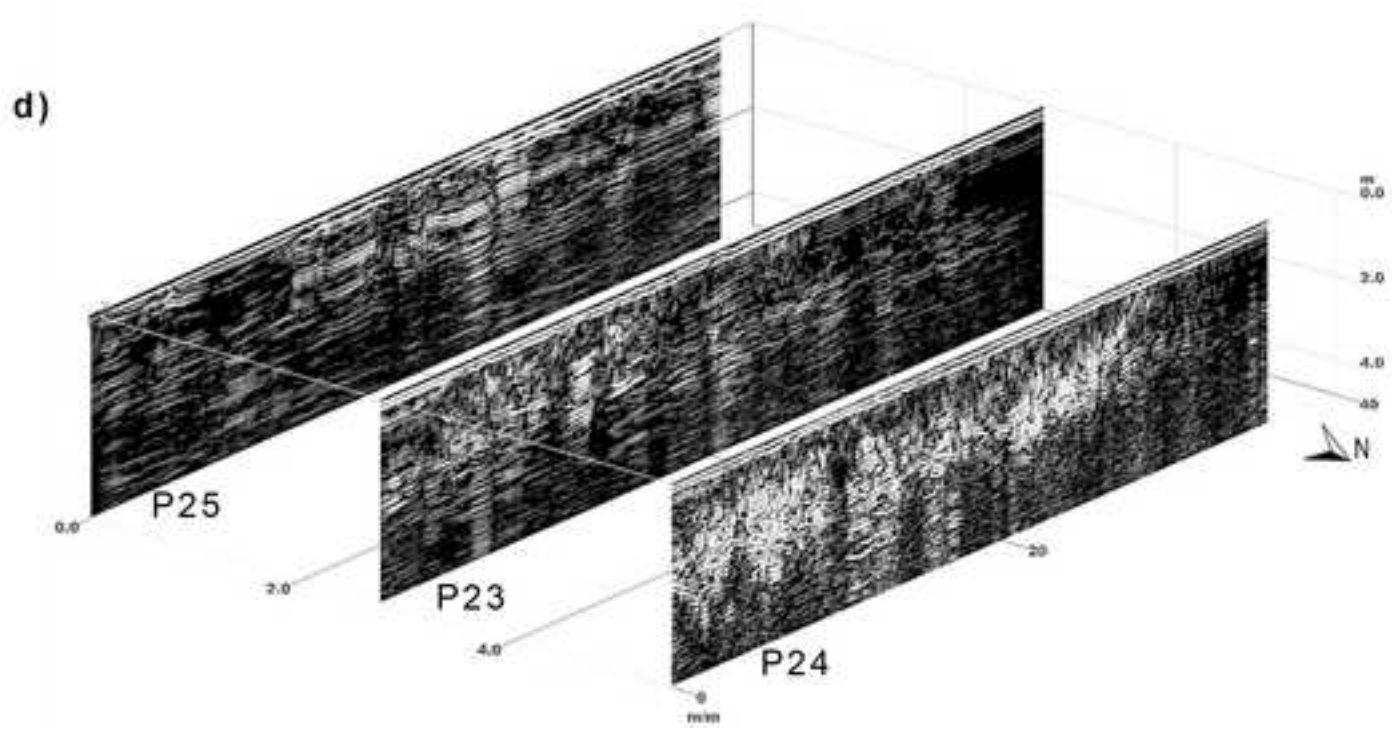
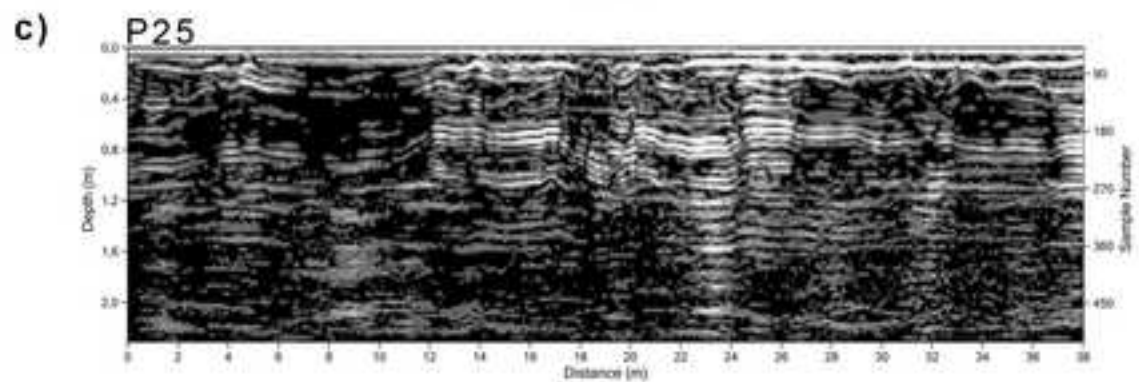
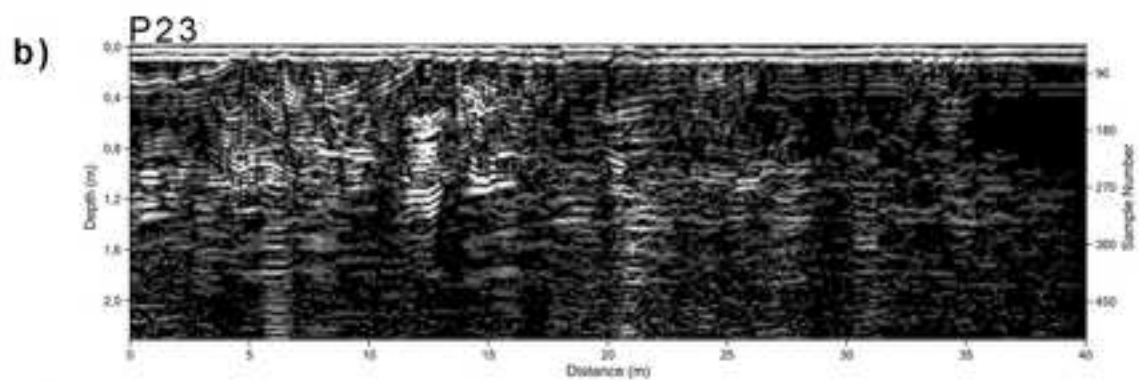
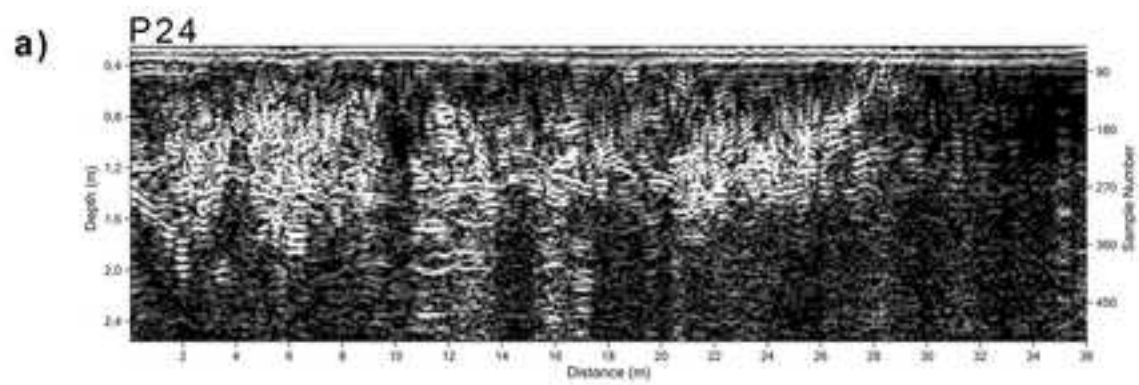


Figure 5  
[Click here to download high resolution image](#)

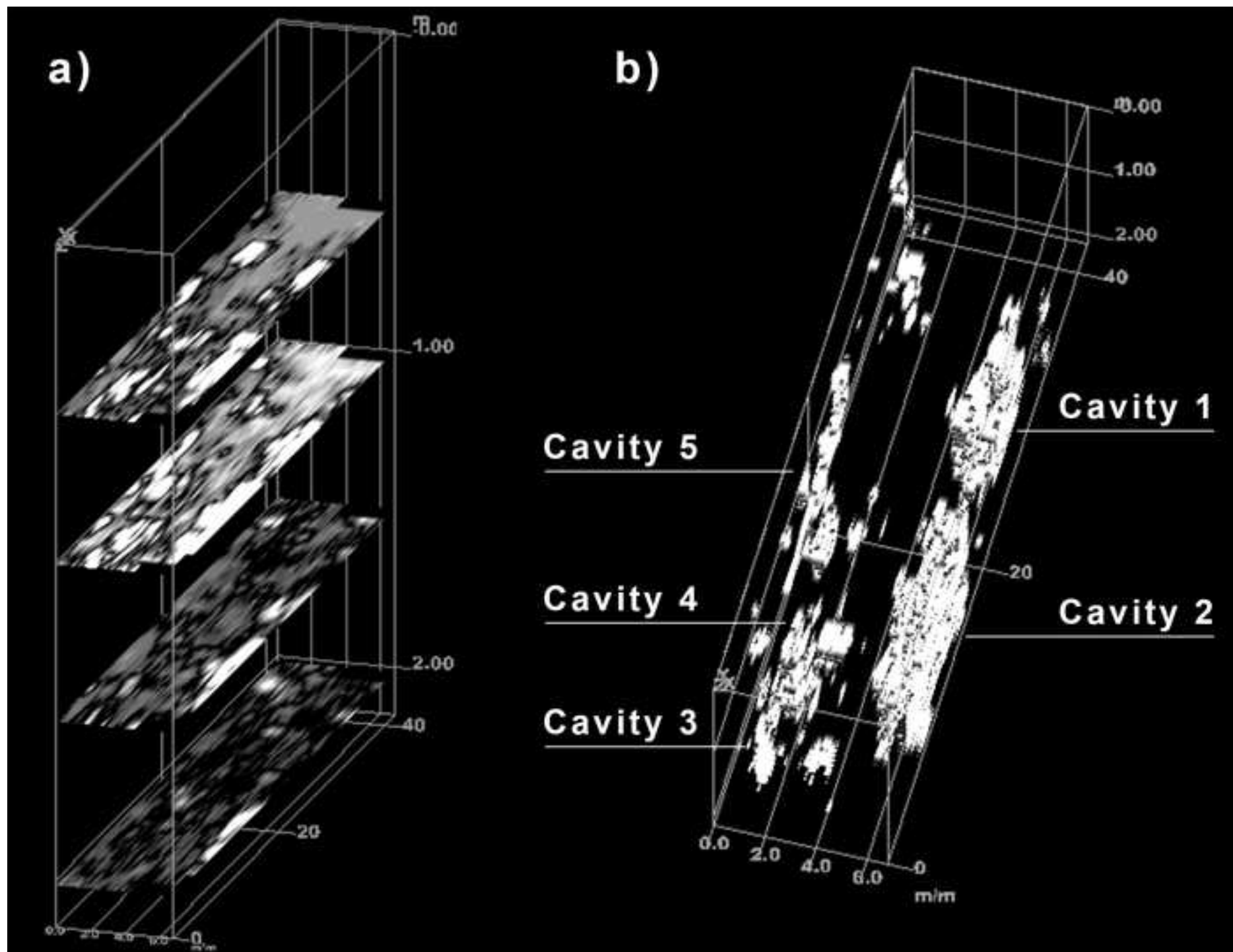


Figure 6  
[Click here to download high resolution image](#)

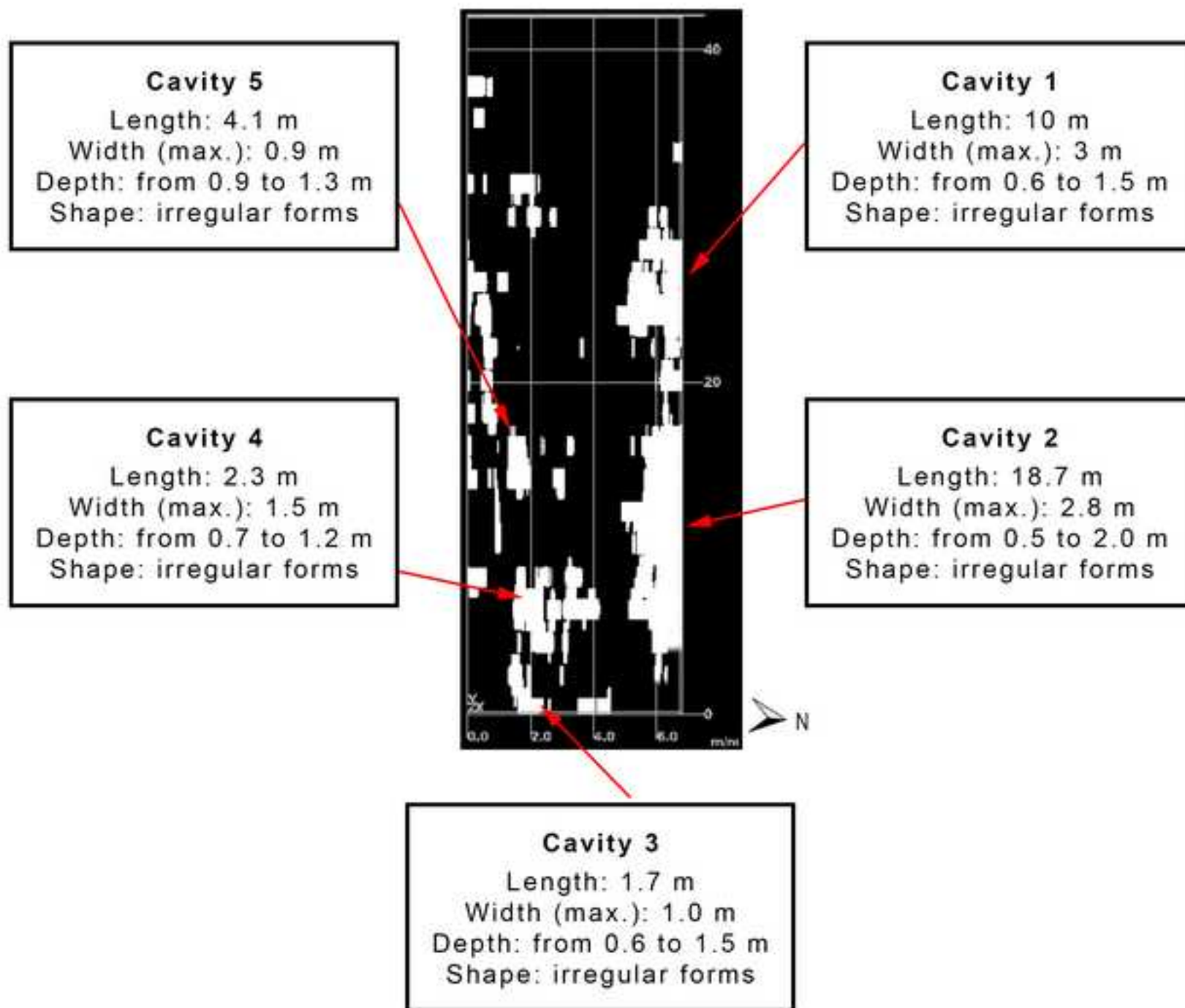


Figure 7  
[Click here to download high resolution image](#)

